Facile synthesis of nano-structured SnO_2 films and their properties in ethanol gas sensing

Ying Wang[1], Hongbin Yu[1] ✉, Hui Suo[2], Xinhong Wang[3], Ying Lu[1], Suiyi Zhu[1], Xia Yang[1]

[1]*School of Environment, Engineering Lab for Water Pollution Control and Resources Recovery, Northeast Normal University, Changchun 130117, People's Republic of China*
[2]*College of Electronic Science & Engineering, Jilin University, Changchun 130012, People's Republic of China*
[3]*College of Resources and Environment, Jilin Agricultural University, Changchun 130118, People's Republic of China*
✉ *E-mail: yuhb108@nenu.edu.cn*

Published in Micro & Nano Letters; Received on 12th November 2017; Revised on 21st March 2018; Accepted on 23rd April 2018

Four types of nano-structured SnO_2 thin films were synthesised via a facile one-step hydrothermal method on Ti substrate. All the films were prepared by using $SnCl_4$ and NaOH as the precursors with urea, mercaptoacetic acid or sodium citrate as the adjusting reagent. The prepared films were characterised by scanning electron microscope, X-ray diffractometer, X-ray photoelectron spectroscopy (XPS) and their properties in ethanol gas sensing were examined. It was found that addition of organic reagents resulted in the formation of different nano-scaled morphologies, i.e. nanowires, nanonets, transparent nanosheets and nanograsses. The characterisation of XPS indicated that SnO_2 was successfully deposited. The gas sensing experiments revealed that morphologies of the nano-SnO_2 films had a great effect on their gas sensing properties. The possible reasons involved were presented.

1. Introduction: Metal oxides (e.g. SnO_2) have attracted wide attentions due to their high catalytic activity and great potentials in applications in different fields, such as gas sensors [1–4], photocatalysts [5, 6], electrodes [7] and supercapacitors [8, 9]. It has been reported that physical and chemical properties of SnO_2 nanomaterials are significantly affected by their geometric structure and surface area [10–12], which means the nano-structure of SnO_2 materials might contribute to their quantum effect, large surface area and high activities. Therefore, to prepare nano-structured SnO_2 materials with different morphologies has become a hot topic in the field of functional materials research.

Currently, many nano-structured SnO_2 materials with different dimensions have been reported, such as zero-dimensional nanoparticles [13–15], one-dimensional nanoneedles [16] and nanowires [17, 18], two-dimensional nanosheets [9, 19, 20], three-dimensional nanoflowers [21–23], nanonets [24, 25] and microspheres [26]. In order to obtain better nano-structured SnO_2 materials, different preparation methods have been investigated, including spray pyrolysis [13], hot-bubbling synthesis [14] and the most popular method of hydrothermal synthesis [18, 21, 24].

It has been proved that the nano-structured SnO_2 is an excellent gas sensing material [1–4, 11, 12, 15, 16, 19–26]. In general, SnO_2 materials with different nano-structures usually have varied gas sensing properties, such as sensitivity and working temperature. Therefore, this Letter mainly focused on two aspects: one was to develop a facile method to prepare SnO_2 films with unique nano-structures by using urea, mercaptoacetic acid or sodium citrate as the adjusting reagent. The other was to test gas sensing properties of the prepared SnO_2 films.

2. Experiment: Acetone (CH_3COCH_3), hydrofluoric acid (HF), oxalic acid ($C_2H_2O_4{\cdot}2H_2O$), sodium hydroxide (NaOH) and urea ($CO(NH_2)_2$) were obtained from Beijing Chemical Plant. Stannic chloride ($SnCl_4{\cdot}5H_2O$), mercaptoacetic acid ($C_2H_4O_2S$) and sodium citrate ($Na_3C_6H_5O_7{\cdot}2H_2O$) were purchased from Sinopharm Chemical Reagent Co., Ltd. All chemicals and reagents were of analytical grade and used without further treatment.

Prior to the hydrothermal experiments, the substrate Ti sheet was polished with sand papers and degreased with ultrasonic in an acetone and a deionised water bath, respectively, for 10 min before drying under a nitrogen flow. Subsequently, it was etched in boiling oxalic acid (1%, v/v) for 120 min, washed with deionised water and blown dry under nitrogen gas. The Ti sheets were activated in 10 M hydrofluoric acid for 15 min before hydrothermal synthesis of SnO_2 films.

In hydrothermal experiments, 0.0126 mol $SnCl_4{\cdot}5H_2O$ and 0.1000 mol NaOH were dissolved into 50 ml deionised water under stirring condition for 20 min [24]. The mixture was transferred into a 100 ml Teflon-lined stainless-steel autoclave, in which a piece of pre-treated Ti sheet was placed. The sealed autoclave was maintained at 180°C for 12 h. Upon cooling down to room temperature, the SnO_2 films were taken out of the autoclave, washed with deionised water and dried in a desiccator for further experiments (the as-prepared nano-structured SnO_2 films were named as NS). Based on the method mentioned above, other three SnO_2 films with different morphologies could be synthesised by adding 0.0083 mol urea, 0.0070 mol mercaptoacetic acid or 0.0034 mol sodium citrate, respectively, into the precursor of $SnCl_4$ and NaOH (the obtained SnO_2 films were named as NSU, NSM and NSS, respectively).

The SnO_2 films were calcined at 400°C for 2 h at a heating rate of 2°C min^{-1} before testing gas sensing properties. The testing equipment was a static system including two parts. One was examination area, and the other was information processing area. A required concentration of testing gas (100 ppm ethanol) was prepared in the air-filled examination area. The voltage rose steadily with temperature increase at the beginning and then reached a smooth response value. The gas sensing response was demonstrated as R_a/R_g, where R_a and R_g were electric resistance of the sensor measured in the air and in target gases, respectively [4].

The morphologies of SnO_2films were observed with a field emission scanning electron microscope (FESEM). The elemental analysis was identified by X-ray diffractometer (XRD) with Cu Kα irradiation (D/maxZ200PC, Rigaku, Japan) and X-ray photoelectron spectroscopy (XPS) with Al Kα radiation (ESCALAB MK II, VG Scientific, England).

3. Results and discussion: Figs. 1*a–d* show the SEM images of the prepared SnO_2 films. Four different morphologies, i.e. nanowires, nanonets, nanosheets and nanograsses, were demonstrated.

The SnO_2 nanowires with the diameter between 20 and 50 nm were obtained by only using inorganic chemicals of NaOH and $SnCl_4$ as precursors, but significant agglomeration was observed on NS (Fig. 1*a*). Organic reagents were usually used to improve the morphology and structure of nano-materials in hydrothermal synthesis processes. As shown in Fig. 1*b*, the nanowires with an average diameter of 30 nm on NSU prepared with urea added were more uniform. Additionally, these nanowires intertwined with each other to form a three-dimensional nanonet structure. When mercaptoacetic acid was used in the hydrothermal synthesis process, another interesting morphology was produced on NSM (Fig. 1*c*). Many ultrathin nanosheets intercalated into the nanonets, forming a unique three-dimensional nano-structure with a large surface area. The nanosheets were so thin that they were almost semitransparent under observation with FESEM. In the case of NSS, a new SnO_2 film with nanograss morphology was obtained (Fig. 1*d*). Thus, the addition of organic reagents in the hydrothermal process might result in unique nano-structures with better distribution and consistency of nano-materials. Undoubtedly, the specific morphologies and structures at nano-level dramatically increased the specific surface area of the films and benefited heterogeneous catalytic reactions.

The crystal structures of the SnO_2films prepared with different organic reagents added were determined by XRD (Fig. 2). The X-ray diffraction peaks at 2θ of 38.39°, 40.15°, 52.98°, 70.62° and 76.19° could be, respectively, ascribed to the (002), (101), (102), (103) and (112) reflection of the crystal lattice of Ti (JCPDS Card No. 89-3073). The diffraction peaks at 2θ of 16.51°, 23.52° and 27.73° could be, respectively, ascribed to the (200), (220) and (311) reflection of SnO_2 (JCPDS Card No. 33-1374).

In order to identify components of the films prepared and their chemical oxidation states, XPS with high-resolution technique was used, and the spectra were shown in Fig. 3. The acquired survey spectrum included C 1s, O 1s, Sn 3d and Ti 2p for both NSU and NSM (Fig. 3*a*). The detailed spectrum of Sn 3d exhibited two peaks with good symmetry (Fig. 3*b*). The small one at 486.4 eV and the large one at 495.9 eV were assigned to Sn 3d5/2 and Sn 3d3/2, respectively, indicating the existence of Sn^{4+} in the SnO_2 films [17]. The high-resolution Sn 3d spectra of

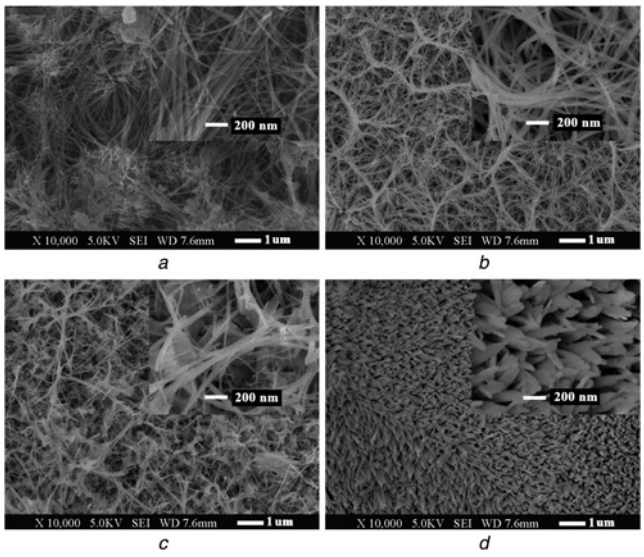

Fig. 1 *SEM images of the films*
a NS
b NSU
c NSM
d NSS
Insets are the magnification images (× 50000)

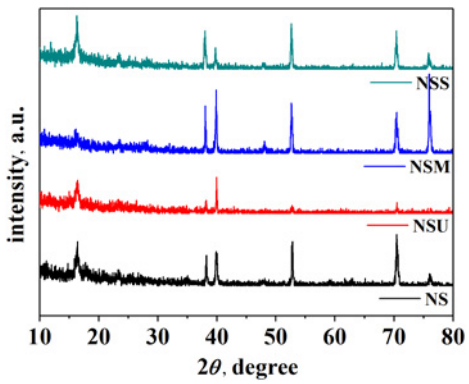

Fig. 2 *XRD patterns of the films*

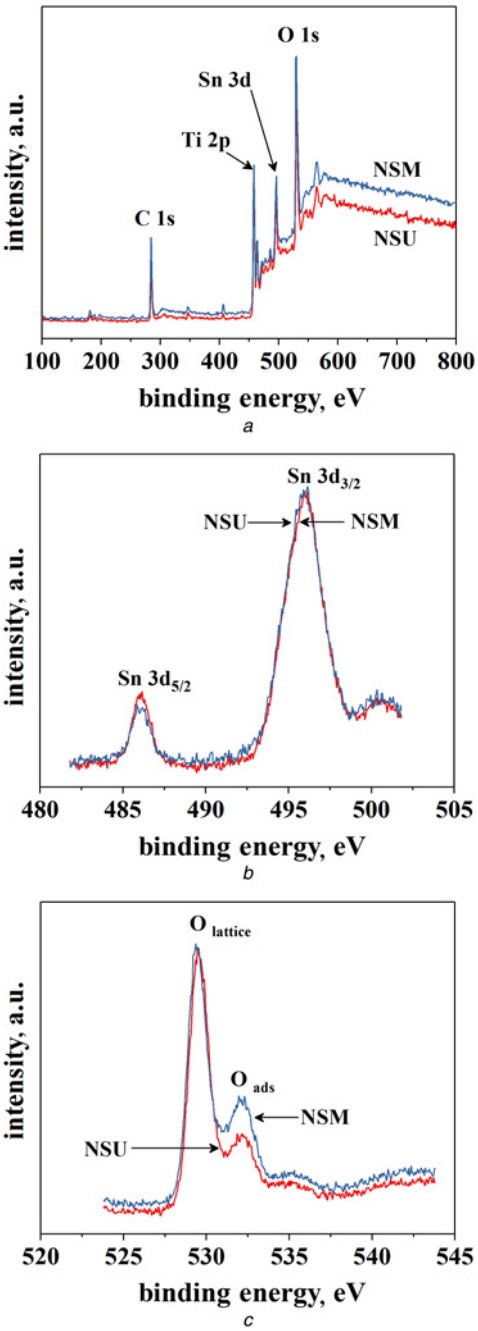

Fig. 3 *XPS analysis for NSU and NSM*
a XPS survey spectrum
b High-resolution spectrum of Sn 3d
c High-resolution spectrum of O 1s

doi: 10.1049/mnl.2017.0806

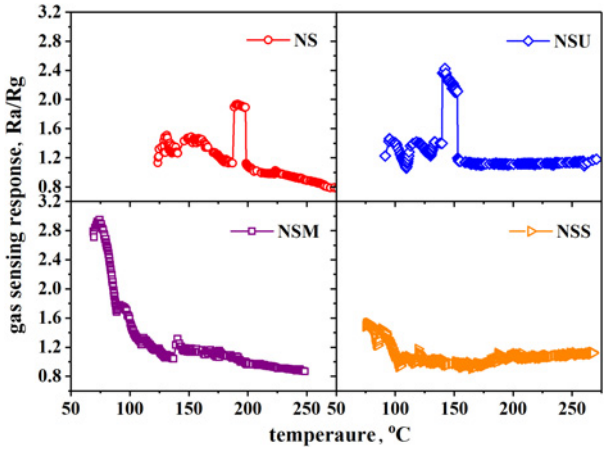

Fig. 4 *Gas sensing response of the SnO_2 films to ethanol (100 ppm)*

NSU and NSM were almost identical, indicating that the oxidation states of tin dioxide in both films were the same. This could be also confirmed by the same binding energy of lattice oxygen ($O_{lattice}$) at 530.1 eV for both films (Fig. 3*c*). The O 1s spectrum of SnO_2 was decomposed into two components. The peak at 530.1 eV was attributed to $O_{lattice}$ of SnO_2, while the peak between 531 and 533 eV was mainly assigned to adsorbed oxygen (O_{ads}) on SnO_2 surface [12, 25, 27]. A higher O_{ads} content in the film of NSM might contribute to its superior ethanol gas sensing properties [12, 25]. This could be confirmed by the gas sensing experiments.

Gas sensing responses of the SnO_2 films were tested with ethanol as the model gas at continuous temperature. In general, the factors of high gas sensing response and low working temperature are two important factors for gas sensors. As reported in the literatures, the morphologies [16, 28] and composition [15] of materials could greatly influence the performance of gas sensors. Similar results were obtained in this work. As seen in Fig. 4, the gas sensing responses and the optimum working temperature were significantly different for the SnO_2films with varied morphologies. Compared with NS, NSU had high gas sensing response and low optimum working temperature, which might be attributed to its higher porosity and specific surface area due to uniform distribution of nanowires (Fig. 1*b*). It was also observed that the gas sensing properties improved further when mercaptoacetic acid was used for hydrothermal synthesis of NSM. The ultrathin nanosheets in the nanonets (Fig. 1*c*) further increased the specific surface area of materials. In addition, the nanosheets interwove with the nanonets, providing more space to force oxygen and ethanol molecules to complete gas sensing reactions due to the confined effect [11]. In contrast, the lowest gas sensing response was observed for NSS, which had more open space on its surface because of the nanograss morphology structure (Fig. 1*d*). Although NSS had low gas sensing response, this unique nanograss structure might be useful as far as photocatalysts were concerned. Additionally, the better gas sensing properties of NSM might also result from its higher O_{ads} content. SnO_2 is known to exchange oxygen from the atmosphere, while oxygen adsorption usually plays a key role in gas sensing. This is because oxygen adsorption can increase resistance of SnO_2 materials due to trapping of charge carriers [29]. When reducing gas species react with adsorbed O_2 (O_{ads}), the trapped electrons are released, thereby increasing the conductivity of the sensor material (SnO_2) [29]. Besides, the nanosheets of NSM might be completely covered by the space charge layer due to its ultrathin nano-structure, and then the grains would be depleted. Thus, the changes of the surface oxygen concentration could significantly affect the conductance of sensor materials [30]. As a result, a higher gas sensing response was obtained for NSM. Therefore, it was concluded that both the O_{ads} content and the nano-structure affected the gas sensing properties of SnO_2.

4. Conclusion: Four types of SnO_2 materials with different nanomorphologies were prepared via a facile one-step hydrothermal method. By adding different organic reagents, the prepared SnO_2 films had varied morphologies, i.e. nanowires, nanonets, nanosheets and nanograsses. The morphology and hierarchical structure influenced the gas sensing properties of SnO_2 dramatically. In addition, the O_{ads} content on SnO_2 surface was another important factor in gas sensing. The study will contribute to the development of SnO_2 materials for gas sensing.

5. Acknowledgments: This work was supported by the National Natural Science Foundation of China (grant nos. 51378098, 51778117, 51578118, 51478095), the Excellent Youth Talents Foundation of Jilin Science & Technology Department (grant no. 20170520079JH) and the Long Term Program in '1000 Talent Plan for High-Level Foreign Experts' (grant no. WQ20142200209).

6 References

[1] Zhang J., Li C., Wang B.: 'Ag-decorated SnO_2 nanorods: microwave-assisted green synthesis and enhanced ethanol gas sensing properties', *Micro Nano Lett.*, 2017, **12**, (4), pp. 245–247
[2] Guo J., Liu X., Wang H., *ET AL.*: 'Synthesis of hollow tubular reduced graphene oxide/SnO_2 composites and their gas sensing properties', *Mater. Lett.*, 2017, **209**, pp. 102–105
[3] Tyagi P., Sharma A., Tomar M., *ET AL.*: 'A comparative study of RGO-SnO_2 and MWCNT-SnO_2 nanocomposites based SO_2 gas sensors', *Sens. Actuators B, Chem.*, 2017, **248**, pp. 980–986
[4] Lian X., Li Y., Tong X., *ET AL.*: 'Synthesis of Ce-doped SnO_2 nanoparticles and their acetone gas sensing properties', *Appl. Surf. Sci.*, 2017, **407**, pp. 447–455
[5] Zhuang Z., Huang F., Lin Z., *ET AL.*: 'Aggregation-induced fast crystal growth of SnO_2 nanocrystals', *J. Am. Chem. Soc.*, 2012, **134**, (39), pp. 16228–16234
[6] Cheng G., Hao T., Ke H., *ET AL.*: 'Controlled growth of SnO_2 nanostructures with small diameters and their photocatalytic properties', *Micro Nano Lett.*, 2013, **8**, (8), pp. 473–475
[7] Liu R., Yang W., Fang H.: 'Performance of SnO_2 carbon nanotube composite electrode materials synthesised by the pechini method', *Micro Nano Lett.*, 2016, **11**, (1), pp. 54–56
[8] Yang Z.L., Zhao S.P., Jiang W., *ET AL.*: 'Carbon-supported SnO_2 nanowire arrays with enhanced lithium storage properties', *Electrochim. Acta*, 2015, **158**, pp. 321–326
[9] Ding S., Wen X., Lou D.: 'Sno_2 nanosheet hollow spheres with improved lithium storage capabilities', *Nanoscale*, 2011, **3**, (9), pp. 3586–3588
[10] Han Y., Wu X., Shen G., *ET AL.*: 'Solution growth and cathodoluminescence of novel SnO_2 core-shell homogeneous microspheres', *J. Phys. Chem. C*, 2010, **114**, (18), pp. 8235–8240
[11] Li T., Zeng W., Long H., *ET AL.*: 'Nanosheet-assembled hierarchical SnO_2 nanostructures for efficient gas-sensing applications', *Sens. Actuators B, Chem.*, 2016, **231**, pp. 120–128
[12] Wang S., Yu W., Cheng C., *ET AL.*: 'Fabrication of mesoporous SnO_2 nanocubes with superior ethanol gas sensing property', *Mater. Res. Bull.*, 2017, **89**, pp. 267–272
[13] Alkhayatt A.H.O., Hussian S.K.: 'Fluorine highly doped nanocrystalline SnO_2 thin films prepared by SPD technique', *Mater. Lett.*, 2015, **155**, pp. 109–113
[14] Ding L., He S., Miao S., *ET AL.*: 'Ultrasmall SnO_2 nanocrystals: hot-bubbling synthesis, encapsulation in carbon layers and applications in high capacity Li-ion storage', *Sci. Rep.*, 2014, **4**, p. 4647
[15] Lin Z., Li N., Chen Z., *ET AL.*: 'The effect of Ni doping concentration on the gas sensing properties of Ni doped SnO_2', *Sens. Actuators B, Chem.*, 2017, **239**, pp. 501–510
[16] Li Y., Liu T., Zhang H.: 'New insight into gas sensing performance of nanoneedle-assembled and nanosheet-assembled hierarchical SnO_2 structures', *Mater. Lett.*, 2016, **176**, pp. 9–12
[17] Kumar R.R., Rao K.N., Rajanna K., *ET AL.*: 'Novel co-evaporation approach for the growth of Sb doped SnO_2 nanowires', *Mater. Lett.*, 2013, **106**, pp. 164–167
[18] Zhao J., Yin J., Hua Z.: 'Synthesis, characterization and optical properties of CdS nanowire/SnO_2 nanoparticle nano-heterostructures', *Mater. Lett.*, 2014, **122**, pp. 237–239

[19] Wang L., Wang S., Wang Y., *ET AL.*: 'Synthesis of hierarchical SnO_2 nanostructures assembled with nanosheets and their improved gas sensing properties', *Sens. Actuators B, Chem.*, 2013, **188**, pp. 85–93

[20] Li Y.: 'A novel snowflake-like SnO_2 hierarchical architecture with superior gas sensing properties', *Physica E*, 2018, **96**, pp. 54–56

[21] Kuang X.L., Liu T.M., Zhang Y.Y., *ET AL.*: 'Urchin-like SnO_2 nanoflowers via hydrothermal synthesis and their gas sensing properties', *Mater. Lett.*, 2015, **161**, pp. 153–156

[22] Yu H., Yang T., Wang Z., *ET AL.*: 'Facile synthesis cedar-like SnO_2 hierarchical micro-nanostructures with improved formaldehyde gas sensing characteristics', *J. Alloys Compd.*, 2017, **724**, pp. 121–129

[23] Zhang W.L., Zeng W., Miao B.: 'Preparation of SnO_2 nanoflower with porous nanosheet via a one-step hydrothermal method', *Mater. Lett.*, 2015, **158**, pp. 377–379

[24] Li X.L., Li X.M., Yang W.J., *ET AL.*: 'Preparation of 3D PbO_2 nanospheres@SnO_2 nanowires/Ti electrode and its application in methyl orange degradation', *Electrochim. Acta*, 2014, **146**, pp. 15–22

[25] Hyun S.K., Sun G., Lee J.K., *ET AL.*: 'Ethanol gas sensing using a networked PbO-decorated SnO_2 nanowires', *Thin Solid Films*, 2017, **637**, pp. 21–26

[26] Gu C., Guan W., Liu X., *ET AL.*: 'Controlled synthesis of porous Ni-doped SnO_2 microstructures and their enhanced gas sensing properties', *J. Alloys Compd.*, 2017, **692**, pp. 855–864

[27] Singkammo S., Wisitsoraat A., Sriprachuabwong C., *ET AL.*: 'Electrolytically exfoliated graphene-loaded flame-made Ni-doped SnO_2 composite film for acetone sensing', *ACS Appl. Mater. Interfaces*, 2015, **7**, pp. 3077–3092

[28] Zhou Q., Chen W., Li J., *ET AL.*: 'Nanosheet-assembled flower-like SnO_2 hierarchical structures with enhanced gas-sensing performance', *Mater. Lett.*, 2015, **161**, pp. 499–502

[29] Chowdhuri A., Singh S.K., Sreenivas K., *ET AL.*: 'Contribution of adsorbed oxygen and interfacial space charge for enhanced response of SnO_2 sensors having CuO catalyst for H_2S gas', *Sens. Actuators B, Chem.*, 2010, **145**, pp. 155–166

[30] Meng F., Hou N., Jin Z., *ET AL.*: 'Ag-decorated ultra-thin porous single-crystalline ZnO nanosheets prepared by sunlight induced solvent reduction and their highly sensitive detection of ethanol', *Sens. Actuators B, Chem.*, 2015, **209**, pp. 975–982

doi: 10.1049/mnl.2017.0806